Sensitivity of Convection Permitting Simulations to Lateral Boundary Conditions in Idealised Experiments

Bodo Ahrens [1], **Nora Leps** [1,2]

[1]Institute for Atmospheric and Environmental Science, Goethe University Frankfurt am Main, Germany
[2]Deutscher Wetterdienst, Offenbach, Germany

Key Points:

- The nesting challenge of convection-permitting climate modelling (CPM) is investigated with idealised simulation experiments
- Nesting the CPM into host simulations with grid-spacing in the grey zone of convection is not better than into coarser simulations
- Fraction of the CPM domain is small suggesting a larger domain even at the expense of CPM grid-spacing coarser than usually accepted

Corresponding author: Bodo Ahrens, `Bodo.Ahrens@iau.uni-frankfurt.de`

Abstract

Limited-area convection-permitting climate models (CPMs) with horizontal grid-spacing less than 4 km are being used more and more frequently. CPMs represent small-scale features such as deep convection more realistically than coarser regional climate models (RCMs), and thus do not apply deep convection parameterisations (CPs). Because of computational costs CPMs tend to use smaller horizontal domains than RCMs. As all limited-area models (LAMs), CPMs suffer issues with lateral boundary conditions (LBCs) and nesting. We investigated these issues using idealised so-called Big-Brother (BB) experiments with the LAM COSMO-CLM (≈ 2.4 km). Deep convection was triggered by idealised hills with driving data from simulations with different spatial resolutions, with/without a deep CP, and with different nesting frequencies and LBC formulations. All our nested idealised 2.4 km Little-Brother (LB) experiments performed worse than a coarser CPM simulation (4.9 km) using a four times larger computational domain, but with only 50% computational cost. A boundary zone of > 100 grid-points of the LB could not be interpreted meteorologically because of spin-up of convection and boundary inconsistencies. A host with grid-spacing in the so-called grey zone of convection (ca. 4 - 20 km) was not advantageous to the LB performance compared to an even coarser host. The LB performance was insensitive to the applied LBC formulation and updating (3-hourly or better). Therefore, our CPM experiments suggested opting for a larger domain instead of a higher resolution even if coarser than usual (i.e., > 4 km). Better preconditioning the convectivity at the CPM inflow boundaries might decrease the spin-up zone's depth.

Plain Language Summary

Recently, very high resolution (grid-spacing < 4 km) so-called convection-permitting climate models (CPMs) were developed, which represent deep convection explicitly. CPMs, however, are computationally very expensive. They need information about the state of the atmosphere at their lateral boundaries from coarser models. This paper investigates the setting of the lateral boundary formulation. We used idealised experiments with grid-spacing of ≈ 2.4 km, where deep convection was triggered by small hills. We found that a CPM boundary zone > 100 grid points can not be interpreted reliably. The boundary data should be given to the CPM every 3 hours or more often. The CPM simulations all performed not as well as a reference simulation on a larger domain with the same high or even two times lower resolution. We tested different resolutions of the driving data for the CPMs and found that driving data from a model in the "grey zone" of convection (about 4 to 20 km) is not advantageous for the CPM performance. We concluded that it often might be better to opt for a larger domain with an unusually coarse CPM resolution (≥ 4 km) than for a smaller domain with grid-spacing < 4 km.

1 Introduction

Regional climate models (RCMs) have been developed with the aim to represent regional scale climate processes better than global climate models (GCMs). With this downscaling of driving global climate projections, results can be applied in regional climate assessments (Giorgi, 2019). The added value of limited–area RCM downscaling is dependent on many factors (like the quality of the driving GCM simulation, consistency of RCM and GCM physics, RCM's domain size, resolution jump, formulation of lateral boundary conditions (LBCs)). The impact of the used nesting approach, i.e. the formulation of LBCs, numerical grid resolution jump from driving GCM to RCM, and the update frequency of driving data, is still under debate (Becker et al., 2015; T. Davies, 2014; Matte et al., 2016; Leps et al., 2019; Li et al., 2020).

The first month-long climate simulations used grid-spacing of 60 km (Giorgi & Bates, 1989). Since then, RCM simulations got more complex, multi-centennial, and used better grid resolutions. In CORDEX (Coordinated REgional Climate Downscaling Experiment), for example, a default grid-spacing of about 50 km was suggested to be used in multiple domains covering all global continents (`https://cordex.org/`, Giorgi et al. (2009)), but finer grid-spacing was already suggested and later on used (e.g., 12 km in EURO-CORDEX, `https://www.euro-cordex.net`, or CORDEX-CORE, Sorland et al. (2021)). This, however, results in RCMs being used in the so-called grey zone of convection, i.e., in a grid-spacing range of about 4 - 20 km. Here, the assumptions of the deep convection parameterisations (CPs) used in climate models are not well fulfilled (Weisman et al., 1997).

Recently, limited-area convection-permitting climate models (CPMs) with grid-spacing below 4 km were developed and successfully applied (Kendon et al., 2012; Ban et al., 2014; Prein et al., 2015; Ban et al., 2021; Purr et al., 2021). These CPMs resolve much of deep convection processes and do not use any deep CP. Because of their spatiotemporal very high resolution, the CPMs are computationally very expensive and at present feasible only over smaller and/or shorter climate periods than RCMs (Ban et al., 2021).

In a convection-permitting simulation with grid-spacing of 2.8 km, Brisson et al. (2015) found an extended spatial spin-up zone at the lateral boundaries, especially at the primary inflow boundary, which the simulated convective systems need to fully develop. They investigated the nesting strategy, and concluded that an additional nesting step in the grey zone of convection with 7 km grid-spacing is not beneficial for the CPM simulation compared to a direct nesting into a driving simulation with grid-spacing of 25 km (i.e. with a resolution jump of about a factor of 10). The simulation experiments by Panosetti et al. (2019) have shown that convective processes are simulated climatologically robust (the simulations achieved bulk convergence) in case of strong orographic forcing (in a domain over the European Alps) and less robust in hilly terrain over Central Germany. They concluded that a coarse-grid CPM with grid-spacing of 4.4 km might be sufficient in the mid-latitudes in cases with strong forcing. Typical grid-spacings in real-data applications, however, are 3 km and finer (as, e.g., in Ban et al. (2021) which evaluates several CPMs over the European Alps).

Figure 1 illustrates the CPM nesting challenge we want to investigate here. The simulated precipitation amounts shown are from RCM and CPM simulations discussed in Purr et al. (2019). The RCM was driven by the European Centre for Medium-Range Weather Forecast Interim Reanalysis (ERA-Interim) from 1979 to 2015 using a European-scale domain with horizontal grid spacing of 0.22° ($\approx$ 25 km). The CPM with a domain over Germany with grid-spacing of 0.025° ($\approx$ 2.8 km) was nested into the RCM simulation laterally nudged towards the driving data using Davies relaxation (H. C. Davies, 1976) using hourly updates of the LBCs provided by the RCM. The CPM simulated about 40 % more precipitation at the 309 most convectively active days in the simulation period. Yet, the CPM simulates less precipitation in a spin-up zone along the primary inflow boundary from the South-West.

This study investigates the challenge of nesting CPM into RCM simulations by using idealised experiments. It explores the dependence of the added value of CPM simulations nested in coarser simulations on resolution jumps (which implies decreasing quality of the coarser driving simulation), LBC update frequencies, and LBC formulation. We aim to provide additional guidance in planning CPM climate simulations.

The following section introduces the idealised simulation experiments applied using a modified Big-Brother experiment design (Leps et al., 2019) and the applied limited-area climate model and its set-up. Section 3 presents and discusses the idealised simulation results. Finally, we summarise and draw conclusions.

Figure 1. Mean daily precipitation of 309 convective days from climate simulations with an RCM (left) and nested CPM (right) in a domain over Germany in the period 1983–2015.

2 Method, Model and Experiments

In this study, we used the modified Big-Brother-Experiment protocol as introduced in Leps et al. (2019). First, an idealised simulation was performed using a large domain with a high, convection-permitting resolution, called the Big-Brother (BB) simulation. This simulation drove, i.e. provided lateral boundary and initialisation conditions for, a simulation on a smaller domain but otherwise the same set-up as the BB set-up. The small domain simulation is called the Little-Brother (LB) simulation and is chosen to have a typical domain size as in studies with realistic simulations (e.g., in Brisson et al. (2021); Purr et al. (2021)). So-called Coarse-Brother (CB) simulations were performed on the BB domain with a coarser resolution to represent input data from a coarser model. CB simulations also drove LB simulations, and the BB simulation was used as the reference for the LB and CB simulations. With this protocol, it was possible to show the impact of nesting, the update frequency, U, of LBCs, and the resolution jump, J, from CB to LB set-ups. The following sub-sections give the details.

2.1 Model and reference Big-Brother set-up

The non-hydrostatic LAM COSMO-CLM (e.g., Rockel et al. (2008)) in version COSMO5.0-CLM7 was applied in idealised test configurations. COSMO-CLM has been used successfully in many climate studies with typical grid-spacings from $\sim 50\,\mathrm{km}$ to convection-permitting scales with grid-spacing of $\mathcal{O}(1\,\mathrm{km})$ (Sorland et al., 2021; Purr et al., 2021). Necessary initial and lateral boundary data were compiled with the pre-processor INT2LM2.0-CLM4.

The reference set-up which was used to perform the reference simulation for later sensitivity experiments is called Big-Brother (BB) set-up. We used a one-moment microphysics scheme and shallow convection is parameterized using the convection scheme after Tiedtke (1989). In the reference simulation no deep CP was used. The used radiation scheme follows Ritter and Geleyn (1992), and the lower boundary condition were provided by the sub-model TERRA (with homogeneous land cover: short grass, roughness length 0.01 m) and turbulence scheme as documented in Doms et al. (2018). The Coriolis force term was switched off in all simulations.

The BB set-up used a horizontal grid-spacing of $0.022°$ ($\approx 2.4\,\mathrm{km}$), 50 vertical levels, numerical time steps of 20 s, and a cartesian simulation domain of 1006×452 grid points (domain area: $\approx 2430\times1100\,\mathrm{km}^2$). This domain size is large enough to host two non-overlapping domains with an order of size typical in CPM studies (e.g., Brisson et al. (2015) or Panosetti et al. (2019)). The BB simulation was run for 24 hours with periodic LBCs (with 6 grid point wide overlapping boundary zones). The simulation orography is mainly flat with twelve Gaussian hills (height = 450 m, half-width = 25 km) in the western part of the domain. These hills are planted into the domain to trigger deep convection in the simulation, but are rather smooth aiming not to provide too strong forcing. They resemble hilly terrain in central Germany and not alpine terrain. Panosetti et al. (2019) have shown that simulations with km-scale grid-spacing are more robust with strong orographic forcing from the European Alps than with weaker central German orographic forcing. The BB domain with the locations of the hills is sketched in Fig. 2.

The simulation was initialised with a Weisman and Klemp (1982)–wind shear profile as implemented by Blahak (2015) with a mean zonal wind speed of 20 m/s above 6 km, potential temperatures/relative humidities of 300 K/1 and 343 K/0.25 at the profile base at 0 m and the tropopause in 12 km, respectively. The zonal speed implies a parcel advection time of $\approx 34\,\mathrm{h}$ from the inflow to the outflow boundary.

Figure 2. Domain of the reference simulation BB (blue) and two nested LB domains (orange). Black dots indicate the locations of the Gaussian hills. The left LB domain is used for the "orographic" and the right one for the "inflow" experiments.

2.2 Coarse-Brother set-up

Five different Coarse-Brother (CB) 24-h simulations were performed with COSMO-CLM, covering the BB domain. Due to the overlapping zone for the periodic boundary conditions, the CB domains are slightly larger than the BB domain (interior domains are identical). Three grid spacings frequently used in RCMs, i.e. 0.11, 0.22, and 0.44°, and additionally 0.044° were used. Thus, the CB simulations are 2, 5, 10, and 20 times coarser than the reference BB simulation. Table 1 summarizes the domain set-ups. The idealised hills were smoothed (yielding lower heights and larger half-widths, but keeping the same volume as in the BB set-up) as is usually the case with coarser model grids.

Following, for example Weisman et al. (1997); Brisson et al. (2017), these CB simulations resolve deep convection partly at best and therefore deep convection processes are usually parameterised here using the Tiedtke (1989) scheme in addition to the shallow convection processes. Later we show results with deep convection switched on and switched off to explore the behaviour of the simulations in the grey zone of convective parameterisations. In addition, we show some results with CP triggering by CAPE threshold instead of low-level moisture convergence threshold which is the default in COSMO-CLM. LBCs and initialization was done as in the BB set-up.

Table 1 gives approximate values of the relative computational processing times for the different CB simulations. The 12-km CB simulation needs only about 1 % computing time compared to the BB reference simulation. Additionally, the CB simulations are also much cheaper in terms of necessary memory resources. The difference in cost of switching on or off the deep CP is negligible.

2.3 Little-Brother set-up

The Little-Brother (LB) simulations were driven by BB and CB simulations in order to quantify the impact of typical scale jumps J between driving and driven simulations (see Tab. 1) and of the update frequency (i.e. the frequency of availability of driving data per day) U. The set-up of numerics and physics of the LB simulations were the same as in the BB simulations, but using different domain size and replacing the periodic LBCs and initialization with driving data provided by the BB and CB simulations.

The LB simulations covered domains of 400×300 grid points (about $980\times730\,\mathrm{km}^2$). Two different LB domain locations within the BB domain were chosen (Fig.2). The western LB domain includes the hills and thus represents a region, where orographic triggering of deep convection occurs. The eastern domain in contrast represents a region, where convective cells are advected into the domain through its lateral boundaries.

We chose typical driving frequencies $U \in \{96, 24, 8, 4\}$/day (every 15 minutes, hourly, 3- and 6-hourly). The available driving data were interpolated linearly in between to provide the necessary LBCs for the LB simulation for every numerical time-step. COSMO-CLM uses the Davies relaxation approach H. C. Davies (1976). Here, all driven variables are prescribed at all lateral boundaries, which means the problem is over-specified (too much information is given at the later boundaries). A sponge zone is introduced to buffer any spurious noise developing at the lateral boundary, where the internal model solution is relaxed toward the driving data. Leps et al. (2019) implemented another approach based on Mesinger (1977) which prescribes less information at the outflow boundaries. We call this approach Mesinger approach. More details on the formulation of the LBCs are given in Leps et al. (2019).

As Tab.1 shows each of the LB simulations costs about 26 % of the reference BB simulation and about twice as much as the 4.9-km CB simulation in terms of processing time.

Table 1. Properties of domains and simulations.

Set-up	grid-spacing	grid points	time step	jump J	processing time
BB	$0.022° \approx 2.4$ km	1006×452	20 s	1	100 %
CB	$0.044° \approx 4.9$ km	506×232	45 s	2	13 %
	$0.11° \approx 12$ km	206×100	90 s	5	1 %
	$0.22° \approx 24$ km	106×56	180 s	10	0.3 %
	$0.44° \approx 49$ km	56×34	300 s	20	0.09 %
LB	$0.022° \approx 2.4$ km	400×300	20 s	1	26 %

2.4 Statistics

The simulations of BB, CBs, and LBs were compared using simple statistics of simulated 15-min precipitation: (i) total sum, and (ii) the spatial mean of the grid-point time series' standard deviation. The latter is called transient–eddy standard deviation in Matte et al. (2017) (used for evaluation of spatial spin-up on limited–area simulations). The ratios of the respective statistics, called *sumr* and *tsdr*, were taken as one-value statistics in the comparisons (as in Ahrens et al. (1998)) with the BB reference values as denominators. Thus, simulations yielding *sumr*, *tsdr* values of one match the reference perfectly well measured by these statistics. If not mentioned otherwise, the comparisons were done for each of the LB domains separately reduced by 15 LB grid-points along the boundaries to avoid direct nesting effects in the boundary zones.

3 Results and Discussion

We show and discuss the reference BB and coarse driving CB simulations first, and then the LB simulations nested into the driving simulations BB and CB with different scale jumps J and of lateral boundary conditions (LBCs) update frequency U.

3.1 Driving Simulations BB, CB

Figure 3 shows the precipitation sum of one simulation day for the reference BB and different coarser CB simulations. The reference BB simulation shows precipitation largely orographically triggered by the Gaussian hills. The impact of the periodic boundary conditions in meridional direction can be seen too. Precipitating systems were not advected to or triggered near the outflow boundary within the simulated 24 h. The Fig. shows two CB simulations with the deep CP switched off. With twice as coarse grid-spacing ($J = 2$, CP = off) the pattern looks similar to the reference yet rougher (with intensified precipitation tracks). As Tab. 2 and Fig. 4 show, this CB simulation reduced the precipitation sum and temporal variability by about 15 % in the orographic domain and by less than 5 % in the inflow domain. The five times coarser CB simulation ($J = 5$, CP = off) shows delayed precipitation triggering and further reduced precipitation amounts and variability, especially in the orographic domain (Tab. 2). For $J = 5$, i.e. with grid-spacing of ≈ 12 km, the mountain drag of the hills with a half-width of 25 km is already largely underestimated by the numerical scheme following L. Davies and Brown (2001). It should be noted that with using COSMO-CLM's sub-gridscale orography parameterisation the degradation of simulation quality with increased grid-spacing would be smaller (Obermann-Hellhund & Ahrens, 2018).

The coarse CB simulations with CP switched on, using low-level moisture convergence triggering produced only up to 56 % ($J = 2$, CP = on) and as little as 22 % ($J = 20$, CP = on) precipitation and even less variability (Figs. 3, 4, and Tab. 2). Thus, the

Table 2. Relative precipitation sums (*sumr*) and relative transient-eddy standard deviations (*tsdr*) of the CB simulations compared to the reference BB simulation in the two evaluation areas in the orographic and inflow LB domains (cf. Fig. 2).

set-up		orographic		inflow	
J	**param.**	**sumr**	**tsdr**	**sumr**	**tsdr**
2	off	84 %	84 %	97 %	96 %
2	on	56 %	38 %	32 %	22 %
2	on(CAPE)	81 %	66 %	47 %	47 %
5	off	43 %	42 %	95 %	89 %
5	on	43 %	25 %	37 %	28 %
5	on(CAPE)	72 %	66 %	52 %	56 %
10	on	45 %	25 %	29 %	17 %
20	on	28 %	17 %	22 %	12 %

simulation with grid-spacing $J = 2$, i.e. ≈ 4.9 km, with CP = on performed much worse than with CP = off. Obviously, the CP reduced instability too much and suppressed grid-scale convective precipitation. The simulation with the grey zone grid-spacings of ≈ 12 and the one with ≈ 24 km were similar with further degradation of simulation quality when increasing grid-spacing to ≈ 49 km. The CB quality was slightly better with orographic forcing than in the inflow evaluation domain without the orographic forcing. Interestingly, simulations with CAPE triggering of convection were better in terms of amount and variability than with moisture convergence triggering in our test set-up, but still convective activity was strongly suppressed as the underestimation of amount and variability by more than 50 % in the inflow domain shows in case of $J = 2$ and CP = on. Additionally, the characteristic precipitation tracks as simulated in the CP = off simulation are not visibly in the CAPE simulations (not shown). Overall, there was a decrease of simulation quality with increasing grid-spacing, and without internal forcing by hills. Here, the limitations of the Tiedtke-like CP will not be further discussed, but its weakness shows less with strong forcing.

The results show that the CB simulations are useful idealised coarse-grid host simulation for the nested LB simulations to be discussed in the following.

3.2 Driven Simulations LB

Next to the quality of the driving simulations, Fig. 4 shows the quality, as measured with *sumr* and *tsdr*, of LB simulations driven by BB and CB simulations, with different LBC update frequencies U. The quality of the output of LB simulations driven by the reference BB (with identical grid in the LB domain) was substantially degraded in comparison to the BB data. The precipitation sum was underestimated by about 30 % and more in both the orographic and the inflow LB domain depending on update frequency U. The transient-eddy variability was underestimated by about 10 % in the orographic domain and up to about 30 % in the inflow domain by the LB simulations with LBC update only every six or three hours ($U = 4$/day or 8/day, respectively), and much better represented with hourly or 15-min updates ($U = 24$/day or 96/day, respectively). The LB results were less sensitive on update frequency in the orographic than in the inflow domain, with orographic precipitation triggered by the hills in the orographic domain and not well inherited from the BB simulation at the inflow boundary.

Figure 5 shows the precipitation sums as simulated in the two LB domains with hourly LBC update ($U = 24$/day). The LB driven by BB simulation in the orographic

Figure 3. Simulated precipitation sum by the reference, BB (top panel), and coarser, CB, simulations. The grid-spacing increases from 0.022° to 0.44° from top to bottom row. The left column shows results with deep convection parameterisation switched off, the right column with deep convection parameterisation switched on. The blue and orange boxes show BB and LB domains, respectively, as in Fig. 2.

Figure 4. Scatter diagram of the BB, CB, and LB simulations' relative precipitation sums (*sumr*) vs. relative transient-eddy standard deviations (*tsdr*) in the two evaluation areas in the orographic (left) and inflow (right) LB evaluation domains (cf. Fig. 2).

domain underestimates the impact of the hills in or near the western, inflow boundary zone. This generates a substantial spin-up zone of about 80-100 grid-points depth. This deep spin-up zone can be seen for all U and is largest for 6-hourly updates (Fig. 6). There is a large overestimation of precipitation by the LB in the western inflow boundary zone. In this zone, inconsistency between the interpolated driving and driven simulations generate disturbances and subsequently rainfall, but here, because of small absolute values, the small absolute errors generated large relative errors. The inflow domain simulation shows the deep spin-up zone too and too much precipitation close to the eastern, outflow boundary (Fig. 5 and 6). This backwatering of inconsistencies and subsequent precipitation near the outflow boundary was observed in real-data regional climate modelling experiments too (see (T. Davies, 2014)). But, again, the BB simulation produced only small precipitation amounts in this region yielding large relative errors. Still, the Figs. indicate that, using prefect driving data even with 15-min LBC update, only approximately the inner 50 % of the domain in zonal direction provided good simulation results.

Nesting in the 0.044°, i.e. $J = 2$, CB simulation with deep CP switched off provided quality comparable to nesting into the reference simulation (Figs. 4, 5 and 6) in the orographic domain. In the inflow domain, there was stronger precipitation overestimation in a deeper zone at the outflow boundary (Fig. 6). Nesting the LB into $J = 2$ with deep CP switched on gave the worst results of all nesting experiments (Fig. 4). The LBs precipitation processes were strongly suppressed (Figs. 5 and 6). Sensitivity to the update frequency is again small in the orographic domain compared to the inflow domain. All the nested LB simulations performed worse averaged over the evaluation domains than the 0.044° CB simulation with deep DP switched off. Additionally, the CB simulation with $J = 2$ spent only 13 % of the computing time while a LB simulation needed 26 % compared to a BB simulation.

Interestingly, LB simulations nested into the CB domain with ≈ 12 km grid-spacing (0.11°, scale jump $J = 5$, and deep CP switched on) did not improve the average results in the orographic domain (Fig. 4). As Fig. 6 shows, the LB simulations suffered damaging spin-up at the inflow boundary of more than 150 grid-points (about 40 % of the zonal domain extent). The results in the inflow domain are slightly better, with enough disturbances provided at the inflow boundary to generate precipitation. Beyond the spin-up region the precipitation amounts are comparably well to nesting into the BB simulation.

The results with CB $J = 10$ are better on average. The domain average results are even comparable to the results by nesting into the BB simulation. But, as Fig. 6 shows the underestimation of precipitation in a somewhat smaller spin-up zone than in case $J = 5$ is compensated by an overestimation deeper into the domain. For the inflow domain with $U = 24$/day and 96/day, precipitation is overestimated substantially (up to 100 %) in a zone of more than 100 grid points at the zonal outflow boundary (Fig. 6).

Surprisingly, in the orographic domain the LB nested into the coarsest CB simulation with a scale jump of $J = 20$ produced the best total precipitation amount (Fig. 4). But, there is an extended spin-up zone underestimation which is later on compensated by overestimation (> 50 % in the central region of the domain, Fig. 6). The mean quality in the inflow nesting experiment was comparable to the other experiments. They all show the degraded quality at the outflow boundary. Still, Fig. 5 gives the impression that the simulated precipitation pattern deviates strongest from the BB pattern. The pattern is dominated by artefacts at the boundaries (compensated by an underestimation in the domain centre, Fig. 5), which can clearly be seen in the $J = 10$ simulation, though to a weaker extent. Therefore, the error compensation ranks the LB results with a scale jump from about 50 km to 2.4 km at the boundaries wrongly best on average.

Figure 5. Simulated precipitation sum by the LB simulations (orographic domain: left orange box, inflow domain: right orange box) using different driving simulations (indicated by precipitation sums surrounding the LB domains). The top row shows the results in the BB and in the CB with $J = 2$ simulations (both with deep convection parameterisation switched off). The panels in the second and third row show LB results with increasing resolution jumps (deep convection parameterisation switched on). The LBC update frequency was hourly ($U = 24$/day).

Figure 6. Meridional mean of the ratio of temporal sums of precipitation *sumr* as simulated with the LBs driven by BB and CB simulations using different Us (rows). The left columns shows the results in the orographic, the right column in the inflow domain. The grey zones were not used in calculation of the mean evaluation statistics (Tab. 2 and Fig. 4).

Figure 7. Meridional mean of the ratio of temporal sums of precipitation *sumr* as simulated with the LBs driven by the CB simulation with $J = 10$ and using $U = 8/\text{day}$. The left columns shows the results in the orographic, the right column in the inflow domain. Two different LBC specification approaches were used: Davies relaxation (solid lines), Mesinger (dashed lines).

Given the shown nesting challenge, we tested, as in Leps et al. (2019) at coarser nesting grid-scales, the Mesinger approach as an alternative to the Davies relaxation approach for LBC specification. As illustrated in Fig. 7, the LB simulations with Mesinger LBCs tended to show less deep spin-up zones in the orographic domain, which fits to a smaller boundary zone and thus better representation of the western hills. But, total precipitation underestimation in the evaluation domain was increased by $5-10\,\%$ compared to simulation with the relaxation approach. In the inflow domain the total precipitation amount was generally even more underestimated ($\approx 15\,\%$). This might be an indication of smaller disturbances near the domain boundaries which later triggered convection. Near the outflow boundary, the effects of driving and driven simulation inconsistencies were simulated in a narrower zone with the Mesinger than with the Davies relaxation approach. Overall, the Mesinger approach performed comparable to the Davies relaxation approach.

4 Summary and conclusions

This paper presented idealised CPM nesting experiments using a modified Big-Brother (BB) experiment design as used before for RCMs in Leps et al. (2019). The model applied, COSMO-CLM, was used in many real data simulations successfully at RCM and at CPM scales. The reference BB simulation used a convection-permitting grid-spacing of 2.4 km. Coarse-Brother (CB) simulations with reduced grid-spacing by factors $J =$ 2 to 20 showed the expected degradation of simulation quality in terms of precipitation sum and temporal variability in two sub-domains, the Little-Brother (LB) domains with and without idealised hills. The CB simulation with $J = 2$ (i.e. grid-spacing 4.9 km) and with deep convection parameterisation switched off (CP = off) performed very well compared to the CB with $J = 2$ and CP = on and compared to the coarser CB simulations. In the discussed idealised set-up, the $J = 5$ simulation also performed better without deep CP.

The LB simulations nested into the BB and the $J = 2$, CP = off, simulations produced up to about 30 % less precipitation than the driving simulations with best results using hourly or 15-min update frequency of the LBCs. In the domain with hills, i.e. with orographic forcing, the LB nesting could not improve the driving CB simulations with $J = 2$ or 5 and CP = on, but the driving simulations with $J = 10$ and 20 and CP = on in domain average. All LB simulations showed a large spin-up zone with precipitation underestimation near the inflow boundaries. The hilly domain LB simulations driven by the coarsest CBs compensated spin-up underestimation by overestimation in the inner parts of the domain. The nested simulations in the flat domain, i.e. without internal orographic forcing, did not inherit convective disturbances from the driving CBs with $J = 10$ and 20 at the inflow boundary. Their relatively good evaluation results were probably due to disturbances because of inconsistencies between driving and driven simulation at the inflow boundary.

These results lead to the conclusion that in our idealised set-up at best only the inner 50 % of the domain in main flow direction, i.e. the inner 200 grid points of 400 grid points in zonal direction, of the LB simulations provided useful information. In other words, a buffer zone of at least 100 grid-points depth along the lateral boundaries has to accepted in CPM simulations. The results are slightly better for hourly or 15-min update frequencies than three-hourly. Six-hourly updates yielded the worst results systematically. Using the Davies relaxation or the Mesinger approach in preparing the LBCs had an only negligible impact on results.

In our set-up, the CB simulation with grid-spacing of 4.9 km, CP = off, performs better than all LB simulations. The forcing by the hilly terrain was seen well in the simulation and advected into the flat sub-domain. Following Panosetti et al. (2019) an even stronger forcing would further improve the relative performance. Additionally, this large-domain CB simulation is computationally about two times cheaper than the small domain LB simulations. Still, the LB simulations perform comparably better than here in real-world applications with stronger and/or additional forcings like surface heterogeneity and frontal systems (cf. Coppola et al. (2020)). But, it is recommended to use a driving model with grid-spacing scales not too deep in the grey zone of convection. Direct nesting into, for example, global ERA5 re-analysis data (Hersbach et al., 2020) and global HighResMIP (Haarsma et al., 2016) or regional CORDEX-CORE (Sorland et al., 2021) simulations with about 30 and 25 km grid-spacing, respectively, is sensible given the results shown here. Depending on the application, opting for a larger domain is better than for higher resolution of the CPM simulation. A 3-hourly or better lateral update frequency should be applied. Finally, better preconditioning of convective activity at the CPM domain's inflow boundary (like preconditioning of eddies in large-eddy simulations, Tabor and Baba-Ahmadi (2010)) might help to decrease the depth of the observed spin-up zone.

Acknowledgments

We thank the Deutscher Wetterdienst (DWD) for providing computational facilities at the DMRZ (Deutsches Meteorologisches Klimarechenzentrum). We thank C. Purr, GUF, for help with Fig. 1, and D. Risto, GUF, for his careful reading of the manuscript and for his valuable comments and suggestions. BA acknowledges support from the European Union's H2020 Research and Innovation Programme under Grant Agreement No 776661 (project SOCLIMPACT).

COSMO-CLM is the community model of the regional climate modelling community, which is freely available for community members (https://www.clm-community.eu). Namelists for reproducing the simulations and the data used for evaluation is available online (http://doi.org/10.5281/zenodo.4553188).

References

Ahrens, B., Karstens, U., Rockel, B., & Stuhlmann, R. (1998). On the validation of the atmospheric model REMO with ISCCP data and precipitation measurements using simple statistics. *Meteorology and Atmospheric Physics*, *68*(3-4), 127–142. Retrieved from `http://link.springer.com/10.1007/BF01030205` doi: 10.1007/BF01030205

Ban, N., Brisson, E., Ahrens, B., Caillaud, C., Coppola, E., Pichelli, E., ... others (2021). The first multi-model ensemble of regional climate simulations at kilometer-scale resolution, part I: Evaluation of precipitation. *Climate Dynamics*. (Accepted)

Ban, N., Schmidli, J., & Schär, C. (2014). Evaluation of the convection-resolving regional climate modeling approach in decade-long simulations. *Journal of Geophysical Research: Atmospheres*, *119*(13), 7889–7907. Retrieved from `http://doi.wiley.com/10.1002/2014JD021478` doi: 10.1002/2014JD021478

Becker, N., Ulbrich, U., & Rupert, K. (2015). Systematic large-scale secondary circulations in a regional climate model. *Geophysical Research Letters*, *42*(10), 4142–4149. doi: 10.1002/2015GL063955

Blahak, U. (2015). *Simulating idelized cases with the cosmo-model (draft version).* (Available at `http://www.cosmo-model.org/content/model/documentation/core/artif_docu.pdf`)

Brisson, E., Demuzere, M., & van Lipzig, N. P. M. (2015). Modelling strategies for performing convection-permitting climate simulations. *Meteorologische Zeitschrift*, *25*(2), 149–163. doi: 10.1127/metz/2015/0598

Brisson, E., Leps, N., & Ahrens, B. (2017). Konvektionserlaubende Klimamodellierung. *promet - Meteorologische Fortbildung*, *99*, 41–48.

Brisson, E., et al. (2021). Contrasting lightning projection using the lightning potential index adapted in a convection-permitting regional climate mode. *Climate Dynamics*.

Coppola, E., Sobolowski, S., Pichelli, E., Raffaele, F., Ahrens, B., Anders, I., ... Warrach-Sagi, K. (2020). A first-of-its-kind multi-model convection permitting ensemble for investigating convective phenomena over Europe and the Mediterranean. *Climate Dynamics*, *55*(1-2), 3–34. Retrieved from `http://link.springer.com/10.1007/s00382-018-4521-8` doi: 10.1007/s00382-018-4521-8

Davies, H. C. (1976). A lateral boundary formulation for multi-level prediction models. *Quarterly Journal of the Royal Meteorological Society*, *102*(432), 405–418. Retrieved from `http://doi.wiley.com/10.1002/qj.49710243210` doi: 10.1002/qj.49710243210

Davies, L., & Brown, A. (2001, apr). Assessment of which scales of orography can be credibly resolved in a numerical model. *Quarterly Journal of the Royal Meteorological Society*, *127*(574), 1225–1237. Retrieved from http://www.ingentaselect.com/rpsv/cgi-bin/cgi?ini=xref{\&}body=linker{\&}reqdoi=10.1256/smsqj.57404 doi: 10.1256/smsqj.57404

Davies, T. (2014). Lateral boundary conditions for limited area models. *Quarterly Journal of the Royal Meteorological Society*, *140*(678), 185–196. doi: 10.1002/qj.2127

Doms, G., Forstner, J., Heis, E., Herzog, H., Raschendorfer, M., Reinhardt, T., ... Vogel, G. (2018). *A description of the nonhydrostatic regional COSMO model part II: physical parameterization (V. 5.05)* (Tech. Rep.). Consortium for Small-Scale Modelling. doi: 10.5676/DWD_pub/nwv/cosmo-doc_5.05_II

Giorgi, F. (2019). Thirty Years of Regional Climate Modeling: Where Are We and Where Are We Going next? *Journal of Geophysical Research: Atmospheres*, 2018JD030094. Retrieved from https://onlinelibrary.wiley.com/doi/abs/10.1029/2018JD030094 doi: 10.1029/2018JD030094

Giorgi, F., & Bates, G. T. (1989, nov). The Climatological Skill of a Regional Model over Complex Terrain. *Monthly Weather Review*, *117*(11), 2325–2347. Retrieved from http://journals.ametsoc.org/doi/10.1175/1520-0493(1989)117{\%}3C2325:TCSOAR{\%}3E2.0.CO;2 doi: 10.1175/1520-0493(1989)117⟨2325:TCSOAR⟩2.0.CO;2

Giorgi, F., Jones, C., Asrar, G. R., et al. (2009). Addressing climate information needs at the regional level: the cordex framework. *World Meteorological Organization (WMO) Bulletin*, *58*(3), 175.

Haarsma, R. J., Roberts, M. J., Vidale, P. L., Senior, C. A., Bellucci, A., Bao, Q., ... von Storch, J.-S. (2016). High Resolution Model Intercomparison Project (HighResMIP v1.0) for CMIP6. *Geoscientific Model Development*, *9*(11), 4185–4208. Retrieved from https://gmd.copernicus.org/articles/9/4185/2016/ doi: 10.5194/gmd-9-4185-2016

Hersbach, H., Bell, B., Berrisford, P., Hirahara, S., Horányi, A., Muñoz-Sabater, J., ... Thépaut, J. N. (2020). The ERA5 global reanalysis. *Quarterly Journal of the Royal Meteorological Society*, *146*(730), 1999–2049. Retrieved from https://onlinelibrary.wiley.com/doi/abs/10.1002/qj.3803 doi: 10.1002/qj.3803

Kendon, E. J., Roberts, N. M., Senior, C. A., & Roberts, M. J. (2012). Realism of Rainfall in a Very High-Resolution Regional Climate Model. *Journal of Climate*, *25*(17), 5791–5806. Retrieved from http://journals.ametsoc.org/doi/10.1175/JCLI-D-11-00562.1 doi: 10.1175/JCLI-D-11-00562.1

Leps, N., Brauch, J., & Ahrens, B. (2019). Sensitivity of limited area atmospheric simulations to lateral boundary conditions in idealised experiments. *Journal of Advances in Modeling Earth Systems*, –(–), accepted. doi: --

Li, S., Li, L., & Le Treut, H. (2020). An idealized protocol to assess the nesting procedure in regional climate modelling. *International Journal of Climatology*, joc.6801. Retrieved from https://onlinelibrary.wiley.com/doi/10.1002/joc.6801 doi: 10.1002/joc.6801

Matte, D., Laprise, R., Thériault, J. M., & Lucas-Picher, P. (2017). Spatial spin-up of fine scales in a regional climate model simulation driven by low-resolution boundary conditions. *Climate Dynamics*, *49*(1-2), 563–574. Retrieved from http://link.springer.com/10.1007/s00382-016-3358-2 doi: 10.1007/s00382-016-3358-2

Matte, D., Laprise, R., Thériault, J. M., & Lucas-Pichier, P. (2016). Comparison between high-resolution climate simulations using single- and double-nesting approaches within the big-brother experimental protocol. *Climate Dynamics*, *47*(12), 3613–3626. doi: 10.1007/s00382-016-3031-9

Mesinger, F. (1977). Forward-backward scheme, and its use in a limited area model. *Beiträge zur Physik der Atmosphäre*, *50*, 200-210.

Obermann-Hellhund, A., & Ahrens, B. (2018). Mistral and tramontane simulations with changing resolution of orography. *Atmospheric Science Letters*, *19*(9), e848. Retrieved from http://doi.wiley.com/10.1002/asl.848 doi: 10.1002/asl.848

Panosetti, D., Schlemmer, L., & Schär, C. (2019). Bulk and structural convergence at convection-resolving scales in real-case simulations of summertime moist convection over land. *Quarterly Journal of the Royal Meteorological Society*, *145*(721), 1427-1443. Retrieved from https://rmets.onlinelibrary.wiley.com/doi/abs/10.1002/qj.3502 doi: 10.1002/qj.3502

Prein, A. F., Langhans, W., Fosser, G., Ferrone, A., Ban, N., Goergen, K., … Leung, R. (2015). A review on regional convection-permitting climate modeling: Demonstrations, prospects, and challenges. *Reviews of Geophysics*, *53*(2), 323–361. doi: 10.1002/2014RG000475

Purr, C., Brisson, E., & Ahrens, B. (2019). Convective shower characteristics simulated with the convection-permitting climate model cosmo-clm. *Atmosphere*, *10*(12), 810. Retrieved from https://www.mdpi.com/2073-4433/10/12/810 doi: 10.3390/atmos10120810

Purr, C., Brisson, E., & Ahrens, B. (2021). Convective rain cell characteristics and scaling in climate projections for Germany. *International Journal of Climatology*, joc.7012. Retrieved from https://onlinelibrary.wiley.com/doi/10.1002/joc.7012 doi: 10.1002/joc.7012

Ritter, B., & Geleyn, J.-F. (1992). A Comprehensive Radiation Scheme for Numerical Weather Prediction Models with Potential Applications in Climate Simulations. *Monthly Weather Review*, *120*(2), 303–325. Retrieved from http://journals.ametsoc.org/doi/10.1175/1520-0493(1992)120{\%}3C0303:ACRSFN{\%}3E2.0.CO;2 doi: 10.1175/1520-0493(1992)120⟨0303:ACRSFN⟩2.0.CO;2

Rockel, B., Will, A., & Hense, A. (2008). The regional climate model COSMO-CLM (CCLM). *Meteorologische Zeitschrift*, *17*(4), 347–348. doi: 10.1127/0941-2948/2008/0309

Sorland, S. L., Brogli, R., Pothapakula, P. K., Russo, E., Walle, J. V. d., Ahrens, B., … Thiery, W. (2021). COSMO-CLM regional climate simulations in the CORDEX framework: a review. *Geoscientific Model Development Discuss.*. Retrieved from https://doi.org/10.5194/gmd-2020-443

Tabor, G., & Baba-Ahmadi, M. (2010). Inlet conditions for large eddy simulation: A review. *Computers & Fluids*, *39*(4), 553–567. Retrieved from https://linkinghub.elsevier.com/retrieve/pii/S0045793009001601 doi: 10.1016/j.compfluid.2009.10.007

Tiedtke, M. (1989). A Comprehensive Mass Flux Scheme for Cumulus Parameterization in Large-Scale Models. *Monthly Weather Review*, *117*(8), 1779–1800. Retrieved from http://journals.ametsoc.org/doi/10.1175/1520-0493(1989)117{\%}3C1779:ACMFSF{\%}3E2.0.CO;2 doi: 10.1175/1520-0493(1989)117⟨1779:ACMFSF⟩2.0.CO;2

Weisman, M. L., & Klemp, J. B. (1982). The Dependence of Numerically Simulated Convective Storms on Vertical Wind Shear and Buoyancy. *Monthly Weather Review*, *110*(6), 504–520. Retrieved from http://journals.ametsoc.org/doi/10.1175/1520-0493(1982)110{\%}3C0504:TDONSC{\%}3E2.0.CO;2 doi: 10.1175/1520-0493(1982)110⟨0504:TDONSC⟩2.0.CO;2

Weisman, M. L., Skamarock, W. C., & Klemp, J. B. (1997). The Resolution Dependence of Explicitly Modeled Convective Systems. *Monthly Weather Review*, *125*(4), 527–548. Retrieved from http://journals.ametsoc.org/doi/10.1175/1520-0493(1997)125{\%}3C0527:TRDOEM{\%}3E2.0.CO;2 doi: 10.1175/1520-0493(1997)125⟨0527:TRDOEM⟩2.0.CO;2

Figure 1.

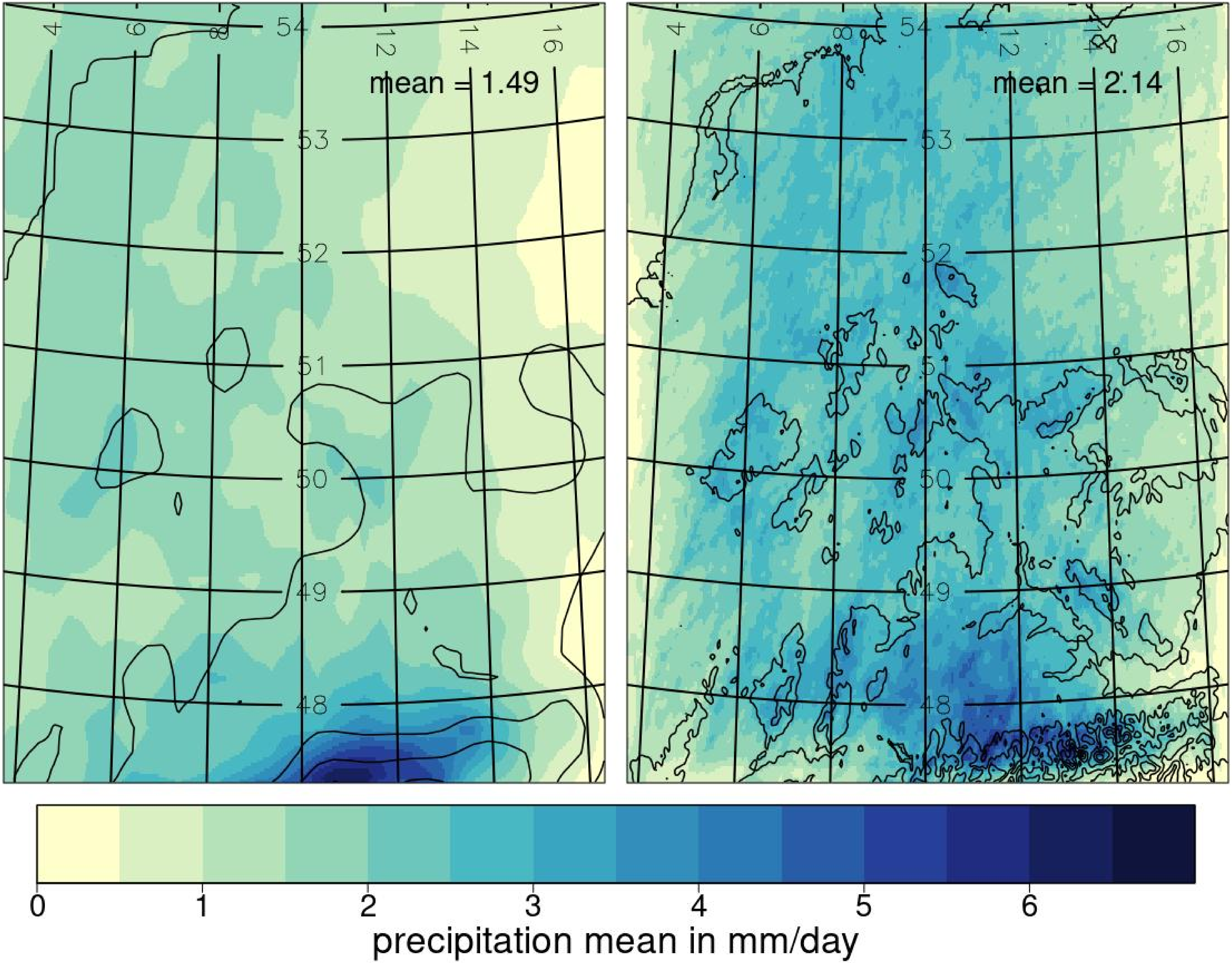

mean = 1.49
mean = 2.14
54
53
52
51
50
49
48
4
6
8
12
14
16
0
1
2
3
4
5
6
precipitation mean in mm/day

Figure 2.

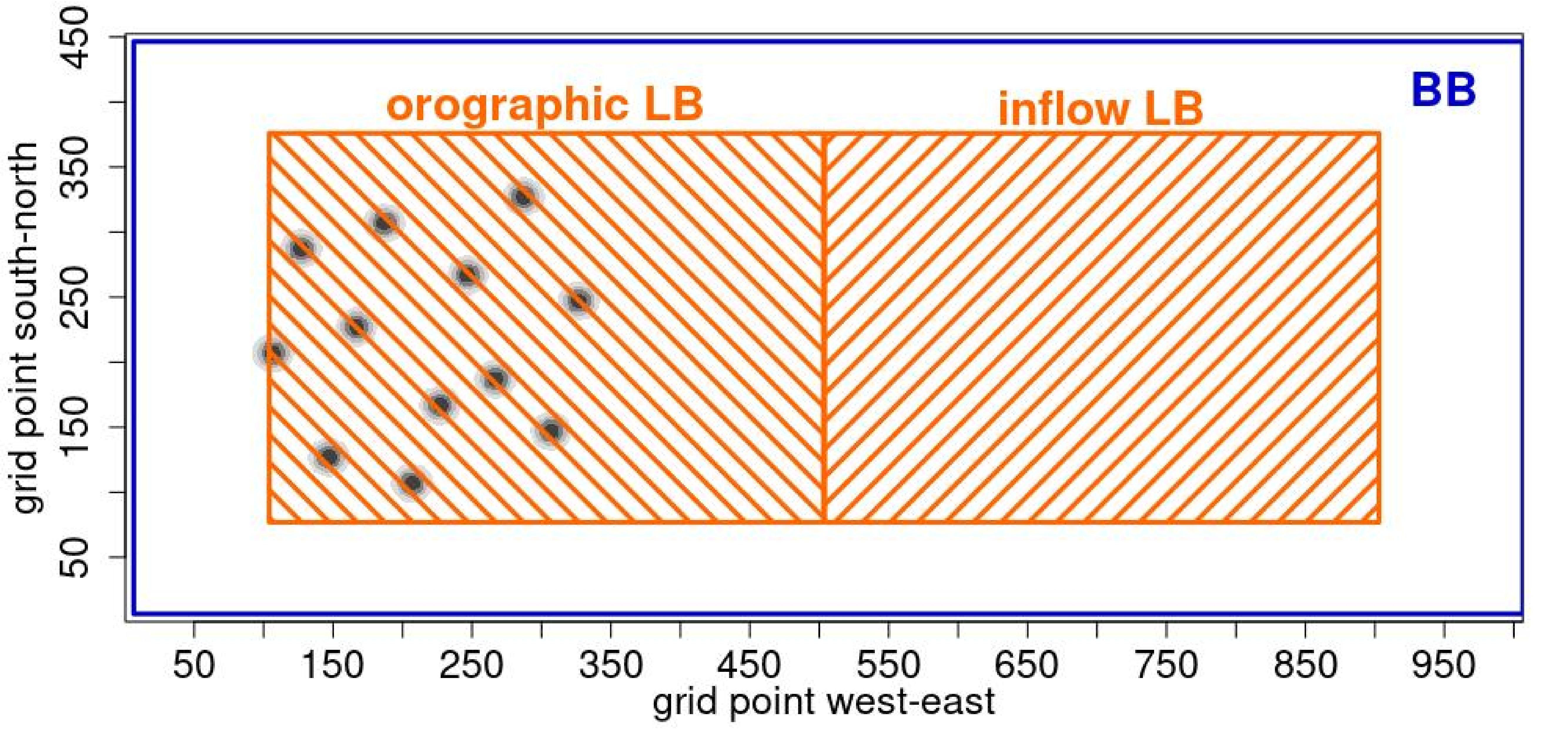

BB
orographic LB
inflow LB
grid point south-north
50
150
250
350
450
grid point west-east
50
150
250
350
450
550
650
750
850
950

Figure 3.

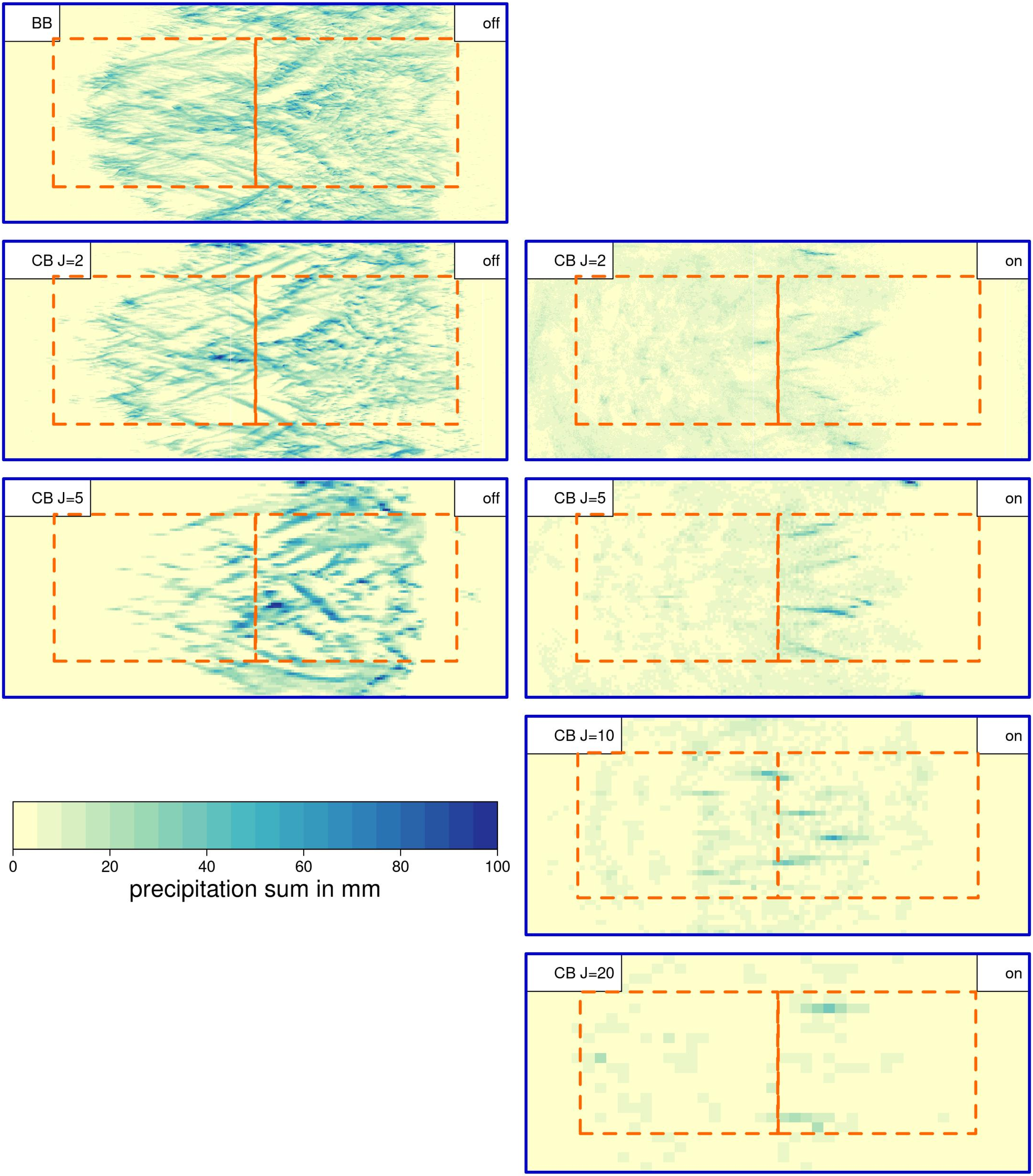
BB
off
CB J=2
off
CB J=2
on
CB J=5
off
CB J=5
on
CB J=10
on
CB J=20
on
0
20
40
60
80
100
precipitation sum in mm

Figure 4.

orographic LB domain
inflow LB domain
J=1 CP off
J=2 CP off
J=2 CP on
J=5 CP on
J=10 CP on
J=20 CP on
BB/CB
LB U=4
LB U=8
LB U=24
LB U=96
sumr [%]
tsdr [%]
20
40
60
80
100

Figure 5.

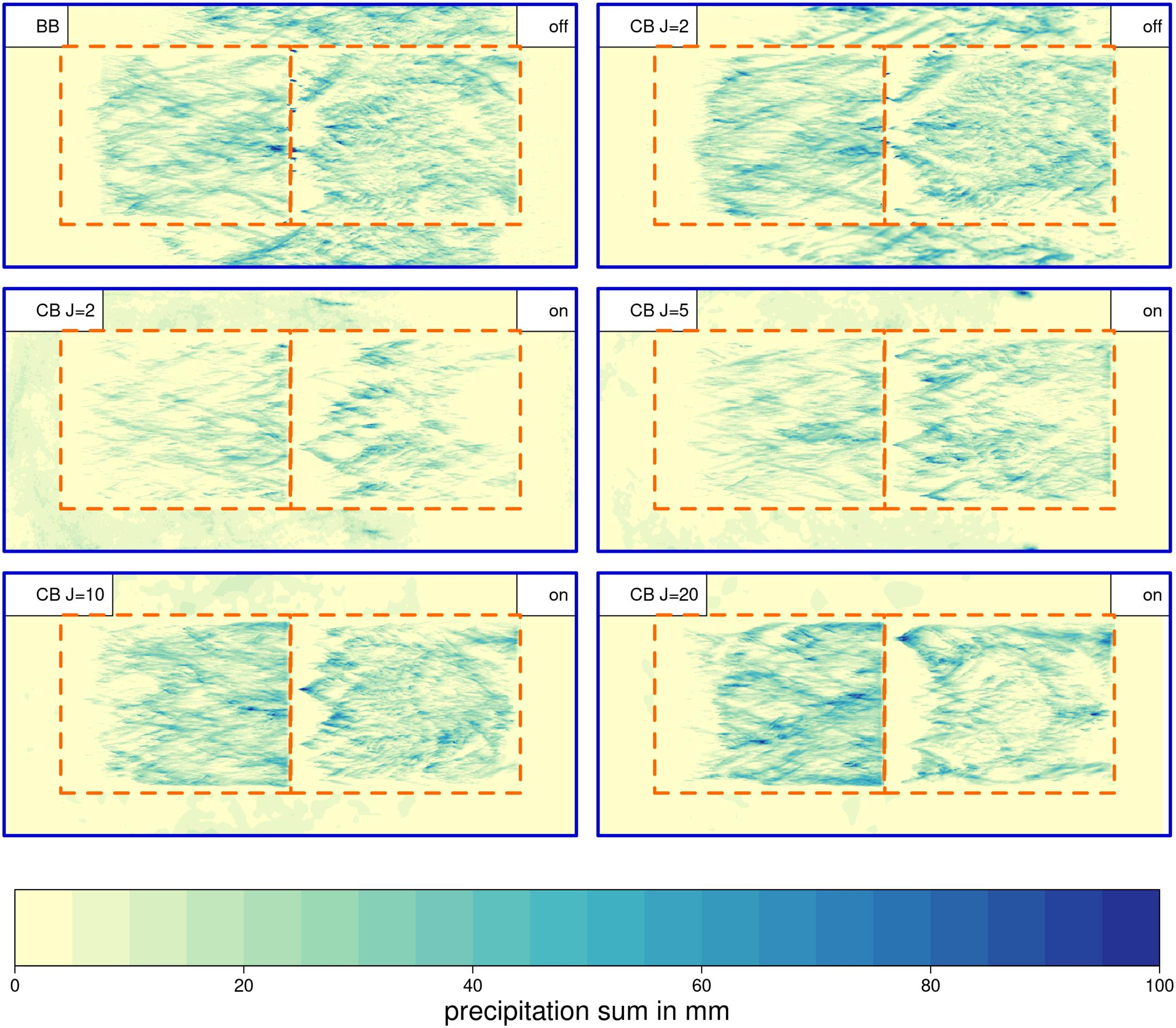

BB
off
CB J=2
off
CB J=2
on
CB J=5
on
CB J=10
on
CB J=20
on
0
20
40
60
80
100
precipitation sum in mm

Figure 6.

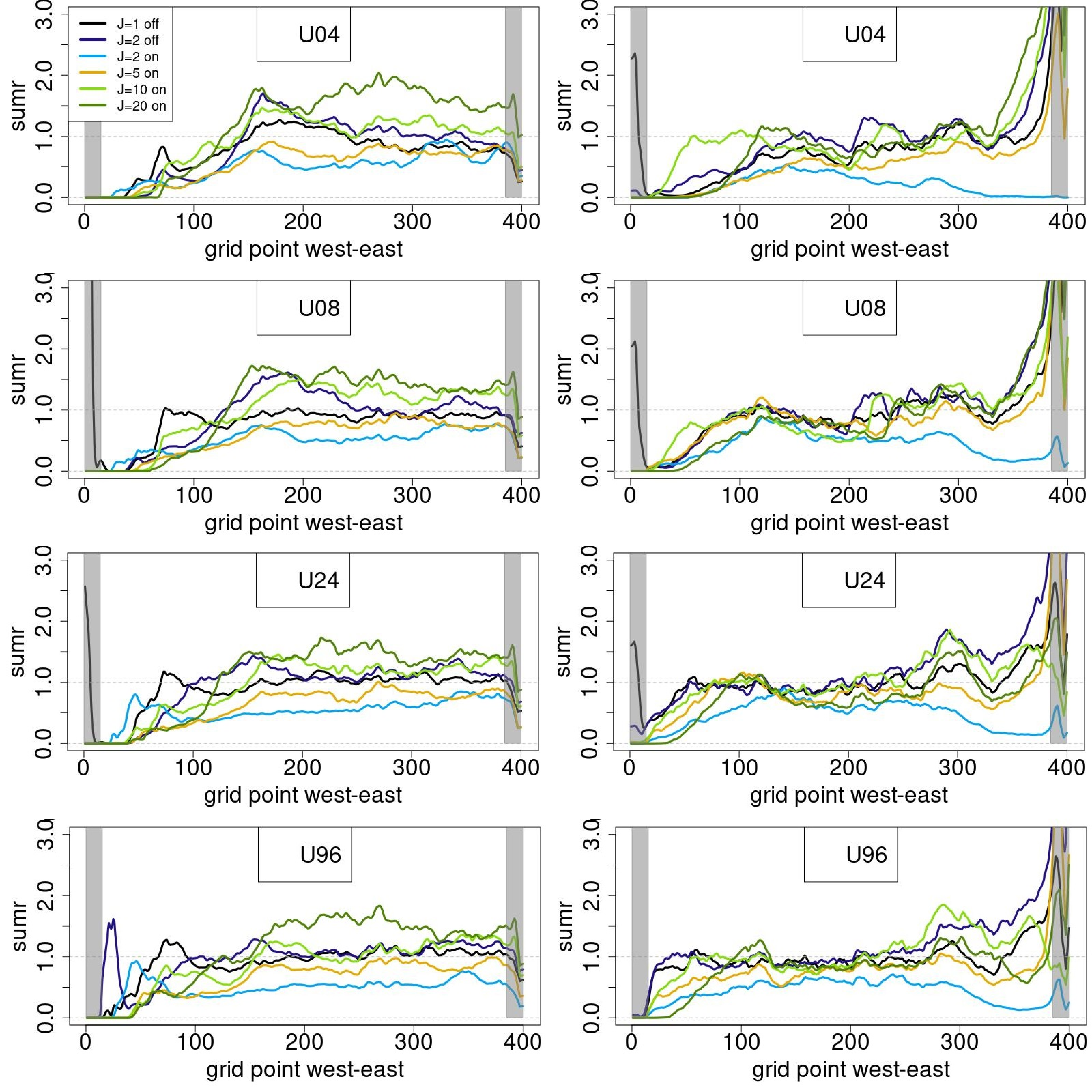
J=1 off
J=2 off
J=2 on
J=5 on
J=10 on
J=20 on
U04
U08
U24
U96
sumr
grid point west-east

Figure 7.

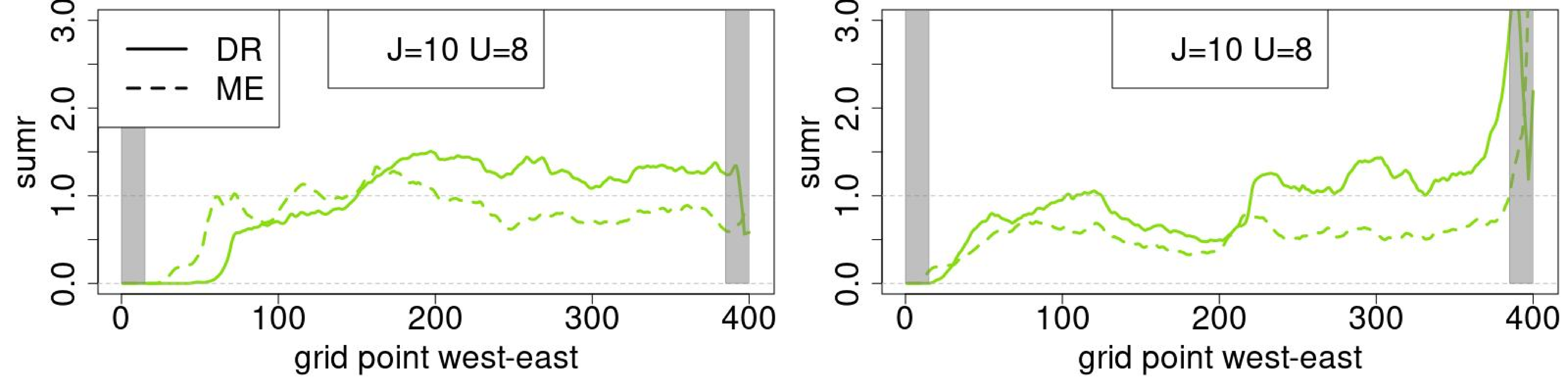

DR
ME
J=10 U=8
sumr
grid point west-east
0.0
1.0
2.0
3.0
0
100
200
300
400
J=10 U=8
sumr
grid point west-east